Biosensors and Bioelectronics 157 (2020) 112160

Contents lists available at ScienceDirect

Biosensors and Bioelectronics

journal homepage: http://www.elsevier.com/locate/bios

An ultrasensitive biosensor for fast detection of *Salmonella* using 3D magnetic grid separation and urease catalysis

Yu Hou [a], Wei Tang [b], Wuzhen Qi [a], Xiaojun Guo [b], Jianhan Lin [a,*]

[a] Key Laboratory of Agricultural Information Acquisition Technology, Ministry of Agriculture and Rural Affairs, China Agricultural University, 17 East Qinghua Road, Beijing, 100083, China

[b] Department of Electronic Engineering, School of Electronic Information and Electrical Engineering, Shanghai Jiao Tong University, Shanghai, 200240, China

ARTICLE INFO

Keywords:
Magnetic nanoparticle chains
Thin-film reference electrode array
Urease catalysis
3D spiral channel
Salmonella detection

ABSTRACT

Screening of pathogenic bacteria plays a crucial role in preventing foodborne disease outbreaks. In this study, an ultrasensitive biosensor was developed for fast detection of *Salmonella* using self-assembled magnetic nanoparticle (MNP) chains for continuous-flow separation of *Salmonella* from large-volume sample, urease coated gold nanoparticles (GNPs) for specific labelling of *Salmonella* and efficient amplification of signal, and linear scan voltammetry for sensitive detection of catalysate. First, MNP chains were formed and distributed in a 3D spiral channel using mutually repelling cylindrical magnets and ring iron gears to control anti-*Salmonella* monoclonal antibody coated MNPs. After bacterial sample was continuous-flow drawn into the channel, bacteria-MNP complexes (magnetic bacteria) were formed on the chains, resulting in specific separation of target bacteria from sample background. Then, anti-*Salmonella* polyclonal antibodies and urease coated GNPs were drawn to label the magnetic bacteria, resulting in the formation of enzymatic bacteria. After washing to remove residual GNPs, urea was drawn and catalyzed by urease on enzymatic bacteria, resulting in the produce of catalysate (ammonium carbonate). Finally, the catalysate was transferred into a microfluidic chip with a thin-film Ag/AgCl reference electrode array for linear scan voltammetric measurement, and the resistance of catalysate was obtained to determine the amount of target bacteria. This biosensor could quantitatively detect *Salmonella* from 1.0×10^1 to 1.0×10^6 CFU/mL in 1 h with low detection limit of 10^1 CFU/mL. The mean recovery for *Salmonella* in spiked milk was about 104.3%.

1. Introduction

Salmonella often ranks the top risk factor for food poisoning and is required for routine screening in monitoring microbial food safety. Existing methods for *Salmonella* detection mainly include culture, polymerase chain reaction (PCR) and enzyme-linked immune-sorbent assay (ELISA), etc. They either require 2–4 days to obtain final results, or need complex DNA extraction procedures, or lack sufficient sensitivity. In recent years, various types of biosensors, such as optical (Banuls et al., 2019; Kaushal et al., 2019; Sekli Belaidi et al., 2019), electrochemical (Bu et al., 2019; Muniandy et al., 2019; Wang et al., 2019) and piezoelectric (Pirich et al., 2017; Shi et al., 2019; Wang et al., 2018), were reported for detection of foodborne pathogens with excellent performance on sensitivity, time and/or cost, however most of them are still in the stage of lab research. Thus, prevention and control of foodborne disease outbreaks is a huge challenge because rapid screening measures are still insufficient.

At present, the procedure for bacteria detection generally includes sample collection and pre-enrichment, bacteria separation and detection. Since very complex food samples often result in big interferences and very few pathogenic bacteria are present in foods for routine screening, specific separation and efficient concentration of target bacteria have become more and more important to their sensitive and accurate detection. Many efforts have been made to investigate new bacterial separation methods based on immunomagnetic separation (Pirich et al., 2017; Smith et al., 2004). An interesting study on magnetic flow separation was proposed by Lee et al. for rapid separation and sensitive detection of pathogenic bacteria from a large volume of food samples using a 3D-printed cylindrical channel, which was able to detect the target bacteria in minutes with a low detection limit of 10 CFU/mL (Lee et al., 2014). However, a very large amount of immune MNPs were needed for ensuring efficient immunoreaction between target bacteria

* Corresponding author.
E-mail address: Jianhan@cau.edu.cn (J. Lin).

https://doi.org/10.1016/j.bios.2020.112160
Received 15 December 2019; Received in revised form 5 February 2020; Accepted 17 March 2020
Available online 20 March 2020

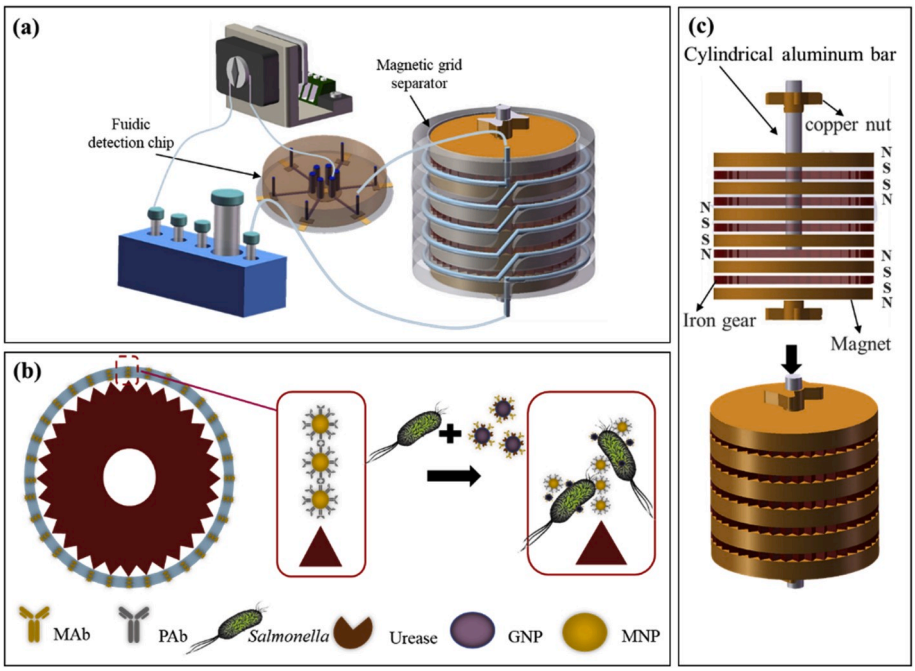

Fig. 1. (a) Structure diagram of the electrochemical biosensor; (b) Principle of magnetic grid separation and gold nanoparticle labeling; (c) Structure diagram of the magnetic grid separator.

and immune MNPs. In recent years, the forming of immune MNP chains in microfluidic channel at the presence of high gradient magnetic field was frequently reported to enhance separation efficiency of target bacteria only using a small amount of MNPs, since biological recognition elements on upright MNPs chains had more chances to react with targets when they flowed through the channel (Luo et al., 2018). A common way to form MNP chains was to set up a permanent magnet at one side of microfluidic channel to generate a gradient magnetic field to capture MNPs (Armbrecht et al., 2015). A typical example for circulating tumor cells sorting was reported by assembling immune MNP chains onto an array of magnetic traps in a microfluidic channel, and more than 94% of target tumor cells were successfully separated (Saliba et al., 2010). Another interesting study on MNP chains was investigated by constructing a magnetic fluidized bed in a microfluidic chip to separate *E. coli* O157:H7 and *Enterobacter cloacae* at the concentrations from 10^2 to 10^7 CFU/mL (Pereiro et al., 2017). However, they both needed very long time (up to 8 h). Thus, new methods for rapid separation and efficient enrichment of target bacteria from large-volume sample are needed to develop sensitive and accurate detection technologies.

Except for specific separation and efficient enrichment of target bacteria from food samples, biological signal amplification also plays an important role in sensitive detection of target bacteria. Many strategies have been attempted to amplify biological signals for enhancing the sensitivity of various detection methods. Among them, enzymes are often employed to amplify the signals, and their catalytic reaction generally requires appropriate conditions (such as pH, temperature, etc.) and well-trained technicians due to complex procedures (Bucur et al., 2018; Elsebai et al., 2017; Wu et al., 2018). Recently, an interesting strategy was reported by Sun et al. for simple, rapid and colorimetric detection of *E. coli* O157:H7 and *Salmonella* typhimurium based on bacterial inhibition of glucose oxidase catalytic reaction (Sun et al., 2019). The total analysis time was less than 20 min, however its lower limit detection was too high (10^4 CFU/mL). In addition, with fast development of microfluidics, many efforts have been made to develop various microfluidic devices for detection of foodborne pathogens (Cai et al., 2018; Kearns et al., 2019). An interesting example was a microfluidic device integrating 3D printing sensing electrodes for contactless conductivity measurement of *E. coli* cells (Duarte et al., 2019). Thus, the combination of microfluidics, MNP chains and enzymatic catalysis might be a promising way to develop new biosensing methods for rapid and sensitive detection of foodborne pathogenic bacteria.

Based on our previous research on exploring high gradient magnetic fields to form MNP chains for bacterial separation (Cai et al., 2018; Wang et al., 2020), this study first constructed a new multi-layer dot--array high gradient magnetic field using six mutually repelling cylindrical magnets and five ring iron gears to form immune MNP chains in a 3D spiral channel. The MNP chains were then used for continuous-flow separation of target bacteria from large-volume sample to form MNP-bacteria complexes (magnetic bacteria) in the channel. After the magnetic bacteria were labelled with immune gold nanoparticles (GNPs) coated with urease, urea was drawn into the channel and catalyzed by urease into catalysate (ammonium carbonate). Finally, linear scan voltammetry was applied to measure the catalysate using a thin-film Ag/AgCl reference electrode array for determination of target bacteria. As illustrated in Fig. 1, this biosensor consisted of two parts: (1) a magnetic grid separator containing a multi-layer high gradient magnetic field and a 3D spiral channel, and (2) a fluidic detection chip containing six thin-film Ag/AgCl reference electrodes and one common reference electrode. The photo of this biosensor could be found in Fig. S1.

2. Materials and methods

2.1. Materials

The anti-*Salmonella* monoclonal antibodies (MAb) from Abcam (ab69255, Cambridge, MA) and the anti-*Salmonella* polyclonal antibodies (PAb) from Meridian (C86309M, Memphis, TN) were employed for specifically reacting with the target *Salmonella* cells. The 150 nm streptavidin conjugated MNPs from Ocean Nanotech (MHS-150-10, San Diego, CA) were used for immunomagnetic separation of target bacteria. Phosphate buffered saline (PBS, 10 mM, pH 7.4), bovine serum albumin (BSA), urease (E.C.3.5.1.5, 15,000–50,000 units/g solid), urea (NH_2CONH_2), and 2-(N-morpholino) ethanesulfonic acid (MES) were purchased from Sigma (St. Louis, MO). Gold chloride tri-hydrate ($HAuCl_4{\cdot}3H_2O$) from Sigma was used to synthesize the GNPs. Ferric

chloride ($FeCl_3 \cdot 6H_2O$) from Macklin (Shanghai, China) was used to prepare the reference electrodes. Polyethylene glycol (PEG) 20,000 from Merck (Darmstadt, Germany) was prepared for blocking. Tween-20 from Amresco (Solon, OH) was used for washing the non-specific binding impurities. The deionized water produced by Millipore Advantage 10 (18.2 MΩ cm, Billerica, MA) was used to prepare all the solutions. The 3D printer (Object 24) and the printing material (Vero Whiteplus RGD835) from Stratasys (Eden Prairie, MN) were used for fabricating the mold of fluidic chip.

2.2. Development of the magnetic grid separator

As shown in Fig. 1, the magnetic grid separator consisted of two parts: a multi-layer high gradient magnetic field and a 3D spiral channel. The high gradient magnetic field was generated using six mutually repelling cylindrical magnets with a thickness of 5 mm and a diameter of 40 mm and five ring iron gears with a thickness of 2 mm and a diameter of 40 mm. A ring gear was placed between each two repelling magnets. These repelling magnets were locked tightly using a cylindrical aluminum bar and two copper nuts. The spiral channel was constructed using a 3D-printed holder to house a Teflon tubing with an outer diameter of ~1.5 mm and a thickness of ~0.25 mm. The MNPs, bacterial samples and the GNPs were successively drawn into the channel at a controllable rate using a precise peristaltic pump.

2.3. Fabrication of the fluidic detection chip

As shown in Fig. S2, the fluidic detection chip was fabricated using screen printing on a glass substrate. First, a layer of conductive nano-silver ink (Hisense Electronics, Suzhou, China) was screen printed onto a clean glass substrate to form one round Ag electrode with a diameter of 5 mm in the center and six rectangle ones (2 mm × 8 mm) in the periphery, followed by curing at 100 °C for 10 min. Then, the Ag/AgCl reference electrodes were formed by dropping 0.1 mol/L ferric chloride to cover the electrodes and incubating for 2 min. After washing with deionized water and drying by nitrogen gas, the glass was treated using oxygen plasma and finally bonded with a PDMS fluidic channel, which was peeled from the 3D printed mold, to obtain the fluidic detection chip. This chip could be used for six measurements.

2.4. Culture and enumeration of the bacteria

Salmonella typhimurium was used as target bacteria. *Escherichia coli* O157:H7, *Cholera*, *Listeria monocytogenes*, *Salmonella* derby and *Salmonella* enteritidis were used as non-target bacteria in this study. For bacterial culture, they were cultured in the Luria-Bertani (LB) medium (Aoboxing Biotech, Beijing, China) at 37 °C for 12–16 h with shaking at 180 rpm, respectively, and their cultures were serially diluted with the sterile PBS to obtain the bacterial cultures with the concentrations from 10^1 to 10^6 CFU/mL. For bacterial enumeration, the bacterial samples were first serially diluted with PBS, then plated on the LB agar plates, and finally incubated at 37 °C for 24 h to count the visible colonies.

2.5. Detection of the target bacteria

The immune MNPs and GNPs were prepared according to our previous reported protocols (Chen et al. 2015, 2016). As shown in Fig. 1, 25 μg of immune MNPs were first drawn into the spiral channel at the flow rate of 150 μL/min and captured by the high gradient magnetic field to form the MNP chains at different layers of the channel. Then, different concentrations (1.0×10^1 to 1.0×10^6 CFU/mL) of *Salmonella* typhimurium were continuous-flow drawn into the channel at the same flow rate, resulting in the forming of magnetic bacteria on the MNP chains, followed by washing with 500 μL of PBST (PBS containing 0.05% Tween-20) to reduce non-specific binding. After the immune GNPs were drawn into the channel to label the magnetic bacteria, resulting in the

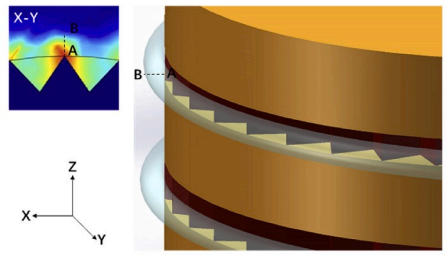

(a)

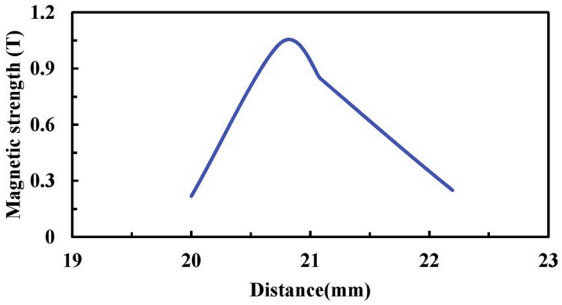

(b)

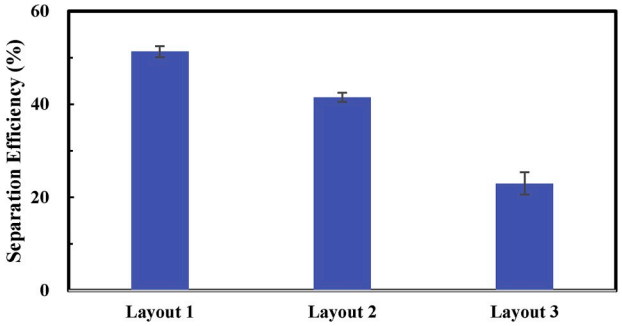

(c)

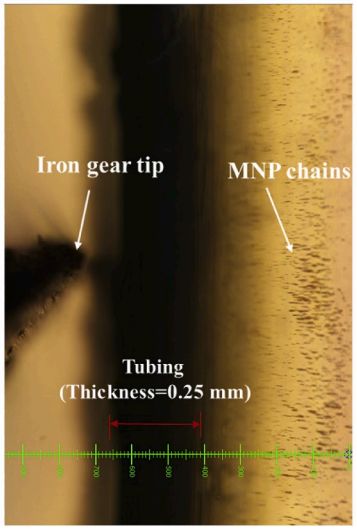

(d)

Fig. 2. (a) Simulation of the magnetic field; (b) The strength of the magnetic field from point A to point B; (c) The separation efficiency of *Salmonella* typhimurium at a concentration of 10^4 CFU/mL using different layouts of magnetic fields (N = 3); (d) The formation of MNP chains in the channel.

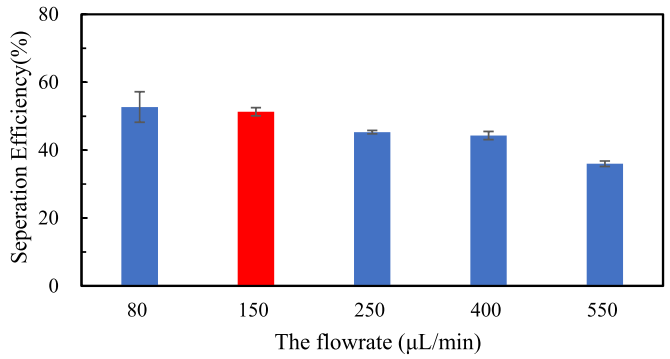

(a)

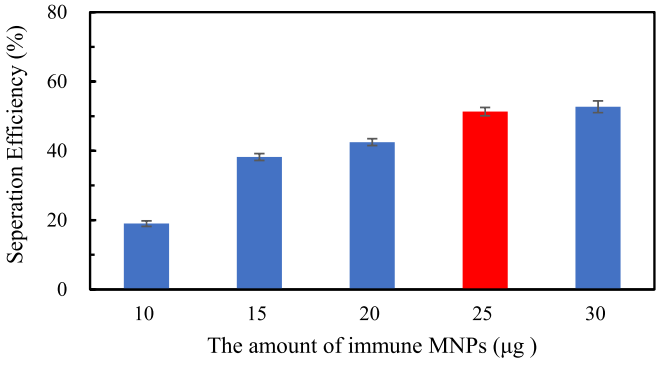

(b)

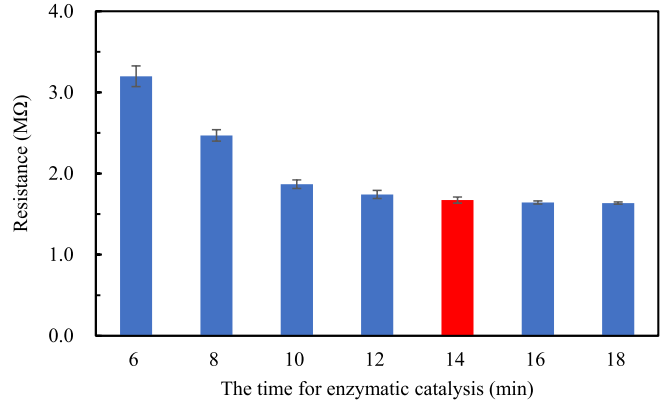

(c)

Fig. 3. (a) Optimization of the amount of immune MNPs; (b) Optimization of the flowrate; (c) Optimization of the time for enzymatic catalysis.

forming of enzymatic bacteria, the channel was washed with PBST again to remove the unbound GNPs. Finally, urea was drawn into the channel and catalyzed by urease on enzymatic bacteria to produce the catalysate, ammonium carbonate, which was drawn into the fluidic detection chip.

2.6. Linear scan voltammetry on the catalysate

After the catalysate (ammonium carbonate) was drawn into one channel of the fluidic detection chip, the thin-film Ag/AgCl reference electrode in the center and the common reference electrode in the periphery were connected by the catalysate, and the linear scan voltammetric measurement of the catalysate was performed using an IM6 electrochemical workstation (Zahner, Kronach, Bavaria, Germany) with the Thales analysis software by applying a linear voltage (U) from 0 to 0.5 voltage with a scan rate of 100 mV/s on these two electrodes. A corresponding current (I) was yielded and could be expressed by Ohm's law as $I=U/R$, where R is the resistance of the catalysate. The resistance of the catalysate is related with the conductivity (ρ) of the catalysate, the length (l) of the channel and the cross-section area (S) of the channel, i.e., $R = \rho l/S$. Since l and S are fixed, R is proportional to ρ. Thus, the concentration of the catalysate was measured and used to determine the amount of target bacteria.

3. Results and discussions

3.1. Simulation of the magnetic field

The magnetic field is the key to the formation of MNP chains in the 3D spiral channel since the magnetic force applied on the MNPs is proportional to the strength and gradient of the magnetic field. Thus, the finite element analysis software COMSOL (Version 5.3a, Burlington, MA) was used to simulate the magnetic field and the simulation results were shown in Fig. 2(a and b). Each layer of magnetic field at the X–Y plane (from the tip of the ring iron gear, point A, to the outer wall of the tube, point B) had a mean gradient of ~0.8 T/mm, allowing the formation of the MNP chains. To verify the effect of the ring iron gears and the mutual repelling layout on separation efficiency of target bacteria, three parallel tests on separation of *Salmonella* typhimurium at 10^4 CFU/mL were conducted using three different layouts: (1) the mutual repelling layout with the ring iron gears, (2) the mutual attracting layout with the ring iron gears, (3) the mutual repelling layout without the ring iron gears. As shown in Fig. 2(c), the separation efficiency for Layout 1 was 51%, higher than those for Layout 2 (42%) and Layout 3 (23%).

The formation of the MNPs chains is crucial to continuous-flow separation of the target bacteria. To verify the formation of MNP chains in the spiral channel at the presence of the magnetic field, a fluorescence inverted microscope (Ti-E, Nikon, Tokyo, Japan) was used to observe the channel from a side view after the MNPs were drawn into the channel at the flow rate of 150 μL/min, followed by standing for 2 min to allow the formation of MNP chains. Fig. 2 (d) demonstrated that the MNP chains were successfully formed in the channel.

3.2. Optimization of the proposed biosensor

The flowrate of the peristaltic pump, the amount of the immune MNPs and the time for enzymatic catalysis have great impact on the sensitivity of this biosensor. First, different flowrates (80 μL/min, 150 μL/min, 250 μL/min, 400 μL/min and 550 μL/min) were used to draw the target bacteria with the concentration of 1.0×10^4 CFU/mL after the MNP chains were formed. As shown in Fig. 3(a), when the flowrate decreased from 550 to 150 μL/min, the separation efficiency of target bacteria gradually increased from 36% to 51%. The further decrease to 80 μL/min did not lead to obvious increase on the separation efficiency. Thus, the optimal flowrate of 150 μL/min was used in this study. Then, different amounts of the immune MNPs were used to capture the target bacteria with the concentration of 1.0×10^4 CFU/mL at the optimal flowrate. As shown in Fig. 3(b), when the amount of the immune MNPs changed from 10 to 25 μg, the separation efficiency increased obviously from 19% to 51%. The further increase to 30 μg did not result in obvious increase on the separation efficiency. Thus, the optimal amount of 25 μg for the immune MNPs was used in this study. Finally, different time for enzymatic catalysis was compared at the optimal conditions for detection of the target bacteria at the concentration of 1.0×10^4 CFU/mL. As shown in Fig. 3(c), when the catalytic reaction time increased from 6 to 14 min, the resistance of the catalysate decreased from 3.20 to 1.67 MΩ, indicating more ammonium carbonate were produced. The further increase to 16 min or more did not have obvious decrease on the resistance. Thus, the optimal time of 14 min for the catalytic reaction was

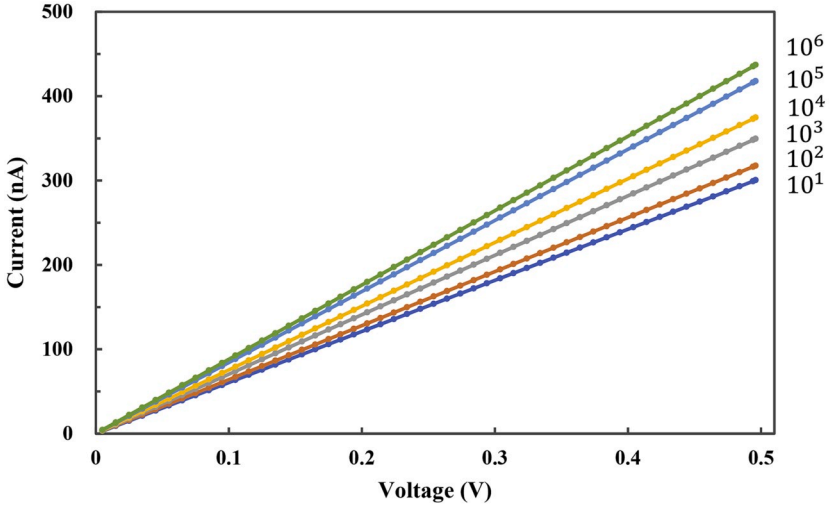

(a)

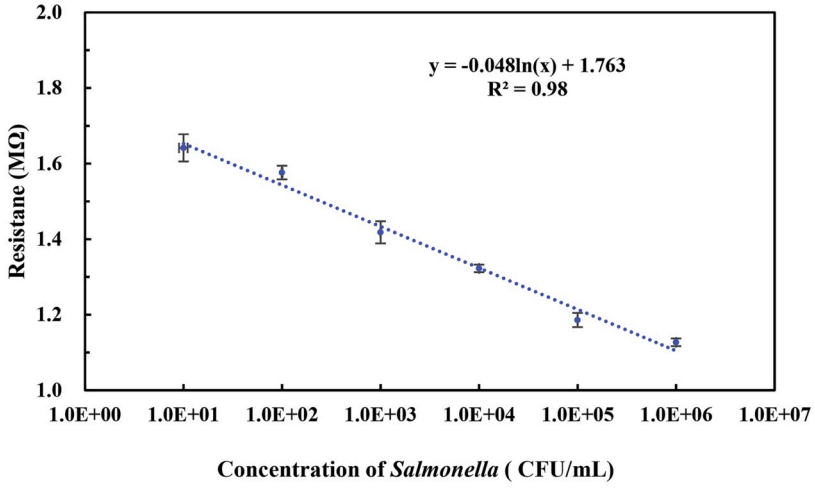

(b)

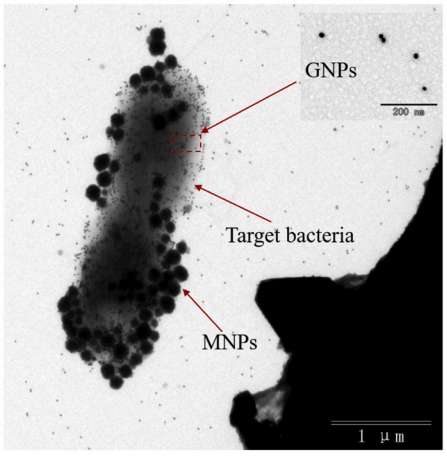

(c)

Fig. 4. (a) The experimental results for linear scan voltammetry; (b)The linear relationship between the resistance of the catalysate and the concentration of the *Salmonella* typhimurium cells from 1.0 × 10^1 CFU/mL to 1.0 × 10^6 CFU/mL (N = 3); (c) TEM image of the enzymatic bacteria.

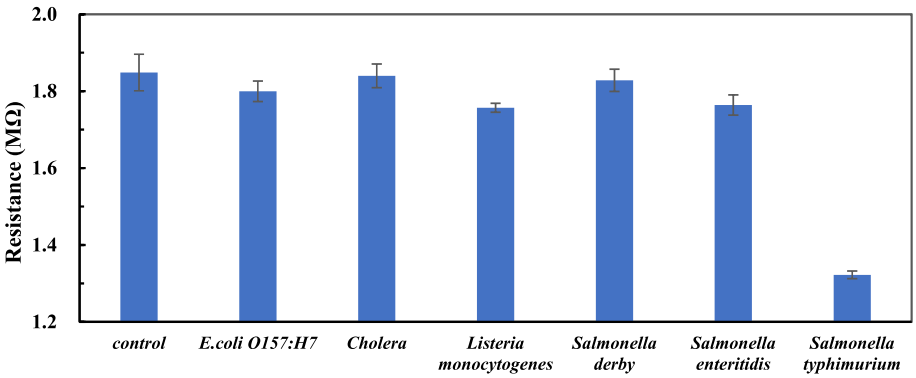

Fig. 5. Detection of *Salmonella* typhimurium, *Listeria monocytogenes*, *Salmonella* derby, *Salmonella* enteritidis, *Cholera* and *E. coli* O157: H7 at the concentration of 10^4 CFU/mL and the negative controls (N = 3).

used in this study.

3.3. Calibration curve of the biosensor for detection of Salmonella

This biosensor was based on linear scan voltammetric measurement of the catalysate for the determination of target bacteria. Thus, it is essential to demonstrate that this voltammetric measurement is feasible to detect the catalysate (ammonium carbonate). To verify this, different concentrations of ammonium carbonate were used to simulate the catalysate and measured using the fluidic detection chip. As shown in Fig. S3, a good logarithmic relationship between the resistance and the concentration was found and could be expressed as $\boldsymbol{R} = -0.642\ln(\boldsymbol{C}) + 0.372$ ($R^2 = 0.98$), indicating that the linear scan voltammetric measurement with these two reference electrodes was applicable for quantitative determination of the catalysate. Besides, the resistance of the substrate (urea) was also measured to be 8.15 MΩ, which was close to that of the deionized water (8.29 MΩ), verifying that urea was almost non-conductive and the resistance change of the urea after urease catalysis was due to the production of ammonium carbonate.

The calibration curve of the biosensor was established by detecting different concentrations of the target bacteria under the optimal conditions. First, 5 mL of different concentrations of the *Salmonella* typhimurium cells ranging from 1.0×10^1 CFU/mL to 1.0×10^6 CFU/mL were magnetically separated using the MNP chains in the 3D spiral channel to form the magnetic bacteria. Then, the magnetic bacteria were labelled with the immune GNPs to form the enzymatic bacteria in the channel. After urea was catalyzed by the urease on the enzymatic bacteria in the channel, the catalysate was drawn into the fluidic detection for resistance measurement. The experimental results for linear scan voltammetry were shown in Fig. 4(a). When the concentration of the target bacteria increased from 10^1 to 10^6 CFU/mL, the current gradually decreased because more enzymatic bacteria were formed and thus more ammonium carbonate were produced within the same catalytic time. As a result, a good linear relationship between the resistance ($\boldsymbol{R}$) of the catalysate and the concentration ($\boldsymbol{C}$) of the *Salmonella* typhimurium cells was found and could be expressed as $\boldsymbol{R} = -0.048\ln(\boldsymbol{C}) + 1.763$ ($R^2 = 0.98$) (see Fig. 4(b)). The detection limit of the biosensor was calculated to be 10^1 CFU/mL according to three times of signal-to-noise ratio. Besides, transmission electron microscope (TEM) imaging was conducted to confirm the successful forming of the urease bacteria and shown in Fig. 4(c).

Compared to some recently reported studies for detection of *Salmonella*, as shown in Table S1, this biosensor has shown a higher or comparable sensitivity and/or a shorter detection time. The high sensitivity of this biosensor could be attributed to the following reasons: (1) The enzymatic catalysis for efficient amplification of the biological signals, resulting in obvious resistance change even for low concentrations of target bacteria; (2) The forming of the magnetic nanoparticle chains in the fluidic channel for continuous-flow separation of target bacteria, resulting in the capture of more bacteria; (3) The reference electrodes for sensitive and accurate measurement of the catalysate, resulting in better background noise control.

Table 1
The recovery of *Salmonella* typhimurium with the concentrations from 1.0×10^1 CFU/mL to 1.0×10^6 CFU/mL.

Salmonella concentration (CFU/mL)	Resistance for pure culture (MΩ)	Resistance for spiked milk (MΩ)	Recovery (%)	Standard deviation (%)
1.0×10^1	1.642	1.644	110.6	4.3
1.0×10^2	1.576	1.500	118.0	4.5
1.0×10^3	1.418	1.417	106.3	2.2
1.0×10^4	1.322	1.339	97.5	1.4
1.0×10^5	1.186	1.226	99.4	1.6
1.0×10^6	1.127	1.141	94.2	1.8

3.4. Specificity of this proposed biosensor

The specificity of the proposed biosensor mainly relied on the anti-*Salmonella* typhimurium monoclonal and polyclonal antibodies. Three parallel tests on negative controls (PBS), *Salmonella* typhimurium, *E. coli* O157: H7, *Listeria monocytogenes*, *Salmonella* derby, *Salmonella* enteritidis and *Cholera* at the same concentration of 10^4 CFU/mL were conducted to evaluate the specificity of this biosensor. As shown in Fig. 5, the resistance for *E. coli* O157: H7 (1.80 MΩ), *Listeria monocytogenes* (1.75 MΩ), *Salmonella* derby (1.82 MΩ), *Salmonella* enteritidis (1.76 MΩ), *Cholera* (1.84 MΩ) and the negative controls (1.85 MΩ) were obviously larger than that of *Salmonella* typhimurium (1.32 MΩ), indicating that the proposed biosensor had a good specificity.

3.5. Application of this biosensor for detection of Salmonella in milk

To further evaluate the applicability of the proposed biosensor, *Salmonella* typhimurium with different concentrations from 1.0×10^1 CFU/mL to 1.0×10^6 CFU/mL were prepared and artificially added into the milk samples which were purchased from the local supermarket and confirmed without *Salmonella* typhimurium. Three parallel tests on the spiked milk samples and the pure cultures using the proposed biosensor were conducted and the results were shown in Fig. S4. The resistances for the spiked milk samples with different concentrations of target bacteria were close to those for the pure cultures at the same concentration. Besides, the recovery of the target bacteria was calculated as the ratio of the readout of the proposed biosensor for the spiked milk sample to that for the pure culture, and shown in Table 1. The recoveries for *Salmonella* typhimurium with the concentrations of 1.0×10^1 CFU/mL, 1.0×10^2 CFU/mL, 1.0×10^3 CFU/mL, 1.0×10^4 CFU/mL, 1.0×10^5

CFU/mL and 1.0 × 10^6 CFU/mL were 110.6%, 118.0%, 106.3%, 97.5%, 99.4% and 94.2%, respectively, and the mean recovery was 104.3%, indicating the feasibility of this proposed biosensor for detection of *Salmonella* typhimurium in milk.

4. Conclusions

In this study, an electrochemical biosensor using self-assembled magnetic nanoparticle chains and enzymatic catalysis was successfully developed for rapid and sensitive detection of *Salmonella* typhimurium. Under the optimal conditions, this biosensor could detect *Salmonella* typhimurium as low as 10^1 CFU/mL within 1 h. The mean recovery for the spiked milk samples was 104.3%, verifying the applicability of this proposed biosensor. The merits of the proposed biosensor mainly include high sensitivity, short detection time and semi-automatic operation. It could be further extended for detection of other foodborne pathogens to enhance food safety by changing the antibodies.

Declaration of competing interest

The authors declare that they have no known competing financial interests or personal relationships that could have appeared to influence the work reported in this paper.

CRediT authorship contribution statement

Yu Hou: Conceptualization, Methodology, Data curation, Formal analysis, Writing - original draft. **Wei Tang:** Resources. **Wuzhen Qi:** Visualization, Software. **Xiaojun Guo:** Resources, Supervision. **Jianhan Lin:** Conceptualization, Formal analysis, Supervision, Project administration, Funding acquisition, Writing - review & editing.

Acknowledgments

This study was supported by National Key Research and Development of China (2016YFD0500903) and Walmart Foundation (SA17031161). The authors would like to thank Walmart Food Safety Collaboration Center for its great support.

Appendix A. Supplementary data

Supplementary data to this article can be found online at https://doi.org/10.1016/j.bios.2020.112160.

References

Armbrecht, L., Dincer, C., Kling, A., Horak, J., Kieninger, J., Urban, G., 2015. Self-assembled magnetic bead chains for sensitivity enhancement of microfluidic electrochemical biosensor platforms. Lab Chip 15 (22), 4314–4321.

Banuls, M.J., Gonzalez-Martinez, M.A., Sabek, J., Garcia-Ruperez, J., Maquieira, A., 2019. Thiol-click photochemistry for surface functionalization applied to optical biosensing. Anal. Chim. Acta 1060, 103–113.

Bu, S.J., Wang, K.Y., Bai, H.S., Leng, Y., Ju, C.J., Wang, C.Y., Liu, W.S., Wan, J.Y., 2019. Immunoassay for pathogenic bacteria using platinum nanoparticles and a hand-held hydrogen detector as transducer. Application to the detection of Escherichia coli O157:H7. Mikrochim. Acta 186 (5), 296.

Bucur, B., Munteanu, F.D., Marty, J.L., Vasilescu, A., 2018. Advances in enzyme-based biosensors for pesticide detection. Biosensors (Basel) 8 (2).

Cai, G., Wang, S., Zheng, L., Lin, J., 2018. A fluidic device for immunomagnetic separation of foodborne bacteria using self-assembled magnetic nanoparticle chains. Micromachines (Basel) 9 (12).

Chen, Q., Lin, J., Gan, C., Wang, Y., Wang, D., Xiong, Y., Lai, W., Li, Y., Wang, M., 2015. A sensitive impedance biosensor based on immunomagnetic separation and urease catalysis for rapid detection of Listeria monocytogenes using an immobilization-free interdigitated array microelectrode. Biosens. Bioelectron. 74, 504–511.

Chen, Q., Wang, D., Cai, G., Xiong, Y., Li, Y., Wang, M., Huo, H., Lin, J., 2016. Fast and sensitive detection of foodborne pathogen using electrochemical impedance analysis, urease catalysis and microfluidics. Biosens. Bioelectron. 86, 770–776.

Duarte, L.C., Figueredo, F., Ribeiro, L.E.B., Corton, E., Coltro, W.K.T., 2019. Label-free counting of Escherichia coli cells in nanoliter droplets using 3D printed microfluidic devices with integrated contactless conductivity detection. Anal. Chim. Acta 1071, 36–43.

Elsebai, B., Ghica, M.E., Abbas, M.N., Brett, C.M.A., 2017. Catalase based hydrogen peroxide biosensor for mercury determination by inhibition measurements. J. Hazard Mater. 340, 344–350.

Kaushal, S., Priyadarshi, N., Pinnaka, A.K., Soni, S., Deep, A., Singhal, N.K., 2019. Glycoconjugates coated gold nanorods based novel biosensor for optical detection and photothermal ablation of food borne bacteria. Sensor. Actuator. B Chem. 289, 207–215.

Kearns, E.A., Gustafson, R.E., Castillo, S.M., Alnughaymishi, H., Lim, D.V., Ryser, E.T., 2019. Rapid large-volume concentration for increased detection of Escherichia coli O157:H7 and Listeria monocytogenes in lettuce wash water generated at commercial facilities. Food Contr. 98, 481–488.

Lee, W., Kwon, D., Chung, B., Jung, G.Y., Au, A., Folch, A., Jeon, S., 2014. Ultrarapid detection of pathogenic bacteria using a 3D immunomagnetic flow assay. Anal. Chem. 86 (13), 6683–6688.

Luo, K., Jeong, K.-B., You, S.-M., Lee, D.-H., Jung, J.-Y., Kim, Y.-R., 2018. Surface-engineered starch magnetic microparticles for highly effective separation of a broad range of bacteria. ACS Sustain. Chem. Eng. 6 (10), 13524–13531.

Muniandy, S., Teh, S.J., Appaturi, J.N., Thong, K.L., Lai, C.W., Ibrahim, F., Leo, B.F., 2019. A reduced graphene oxide-titanium dioxide nanocomposite based electrochemical aptasensor for rapid and sensitive detection of *Salmonella* enterica. Bioelectrochemistry 127, 136–144.

Pereiro, I., Bendali, A., Tabnaoui, S., Alexandre, L., Srbova, J., Bilkova, Z., Deegan, S., Joshi, L., Viovy, J.L., Malaquin, L., Dupuy, B., Descroix, S., 2017. A new microfluidic approach for the one-step capture, amplification and label-free quantification of bacteria from raw samples. Chem. Sci. 8 (2), 1329–1336.

Pirich, C.L., de Freitas, R.A., Torresi, R.M., Picheth, G.F., Sierakowski, M.R., 2017. Piezoelectric immunochip coated with thin films of bacterial cellulose nanocrystals for dengue detection. Biosens. Bioelectron. 92, 47–53.

Saliba, A.E., Saias, L., Psychari, E., Minc, N., Simon, D., Bidard, F.C., Mathiot, C., Pierga, J.Y., Fraisier, V., Salamero, J., Saada, V., Farace, F., Vielh, P., Malaquin, L., Viovy, J.L., 2010. Microfluidic sorting and multimodal typing of cancer cells in self-assembled magnetic arrays. Proc. Natl. Acad. Sci. U. S. A. 107 (33), 14524–14529.

Sekli Belaidi, F., Farouil, L., Salvagnac, L., Temple-Boyer, P., Seguy, I., Heully, J.L., Alary, F., Bedel-Pereira, E., Launay, J., 2019. Towards integrated multi-sensor platform using dual electrochemical and optical detection for on-site pollutant detection in water. Biosens. Bioelectron. 132, 90–96.

Shi, X., Zhang, J., He, F., 2019. A new aptamer/polyadenylated DNA interdigitated gold electrode piezoelectric sensor for rapid detection of Pseudomonas aeruginosa. Biosens. Bioelectron. 132, 224–229.

Smith, L.A., West, J.A., Sobek, D., Hukari, K.W., Renzi, R.F., Patel, K., 2004. Rapid Universal Solublization and Analysis of Bacterial Spores Using a Simple Flow-Through Ultrahigh-Temperature Capillary Device, vol. 5591, p. 56.

Sun, J., Huang, J., Li, Y., Lv, J., Ding, X., 2019. A simple and rapid colorimetric bacteria detection method based on bacterial inhibition of glucose oxidase-catalyzed reaction. Talanta 197, 304–309.

Wang, H., Wang, L., Hu, Q., Wang, R., Li, Y., Kidd, M., 2018. Rapid and sensitive detection of Campylobacter jejuni in poultry products using a nanoparticle-based piezoelectric immunosensor integrated with magnetic immunoseparation. J. Food Protect. 81 (8), 1321–1330.

Wang, L., Huo, X., Zheng, L., Cai, G., Wang, Y., Liu, N., Wang, M., Lin, J., 2020. An ultrasensitive biosensor for colorimetric detection of Salmonella in large-volume sample using magnetic grid separation and platinum loaded zeolitic imidazolate Framework-8 nanocatalysts. Biosens. Bioelectron. 150, 111862.

Wang, Z., Ma, B., Shen, C., Cheong, L.Z., 2019. Direct, selective and ultrasensitive electrochemical biosensing of methyl parathion in vegetables using Burkholderia cepacia lipase@MOF nanofibers-based biosensor. Talanta 197, 356–362.

Wu, Y., Wang, M., Ouyang, H., He, Y., Zhao, X., Fu, Z., 2018. Teicoplanin-functionalized magnetic beads for detection of Staphylococcus aureus via inhibition of the luminol chemiluminescence by intracellular catalase. Mikrochim. Acta 185 (8), 391.